Wavelet Analysis and Synthesis of Fractional Brownian Motion

Patrick Flandrin, *Member, IEEE*

Abstract—**Fractional Brownian motion (fBm) offers a convenient modeling for nonstationary stochastic processes with long-term dependencies and $1/f$-type spectral behavior over wide ranges of frequencies. Statistical self-similarity is an essential feature of fBm and makes natural the use of wavelets for both its analysis and its synthesis. A detailed second-order analysis is carried out for wavelet coefficients of fBm. It reveals a stationary structure at each scale and a power-law behavior of the coefficients' variance from which the fractal dimension of fBm can be estimated. Conditions for using orthonormal wavelet decompositions as approximate whitening filters are discussed, consequences of discretization are considered and, finally, some connections between the wavelet point of view and previous approaches based on length measurements (analysis) or dyadic interpolation (synthesis) are briefly pointed out.**

Index Terms—**Fractional Brownian motion, wavelets.**

I. Introduction

In a large number of physical phenomena, long-term dependencies are involved and $1/f$-type spectral behaviors are observed over wide ranges of frequencies [14]. Although of great importance, the modeling of processes of this type is faced with a number of difficulties which render inadequate the use of conventional approaches such as, e.g., the ARMA approach. Among these difficulties stand the slow decay of the correlation structure associated with long-term dependencies and the fact that $1/f$-type processes have no "natural" description scale.

Nevertheless, a convenient modeling of such processes has been proposed by Mandelbrot and van Ness [20]. It is referred to as *fractional Brownian motion* (fBm) and, among other properties, it possesses that of being statistically self-similar, which means that any portion of a given fBm can be viewed (from a statistical point of view) as a scaled version of a larger part of the same process. Such a property is of course reminiscent of the way in which signals or processes can be described in terms of *wavelets* [5] which are all deduced from one elementary waveform by means of shifts and dilations.

It is, therefore, the purpose of this correspondence to explore some of the links that exist between fBm and wavelets, for both analysis and synthesis purposes. Moreover, it will turn out that the "wavelet point of view" also gives new hints for interpreting previous methods devoted to fBm and for generalizing them.

First attempts for analyzing or synthesizing fBm *via* wavelets go back to [8], [18] and more recent contributions can be found in [27], [25], and [24]. Although it would be equally possible to make use of continuous wavelet representations [8], [25], we will here focus on discrete and orthonormal wavelet decompositions.

II. Fractional Brownian Motion

Fractional Brownian motion (fBm) is a natural extension of ordinary Brownian motion [20]. It is a Gaussian zero-mean nonstationary stochastic process $B_H(t)$, indexed by a single scalar parameter $0 < H < 1$, the usual Brownian motion being recovered from the specification $H = 1/2$.

The nonstationary character of fBm is evidenced by its covariance structure [29]:

$$\mathscr{E}(B_H(t)B_H(s)) = \frac{\sigma^2}{2}(|t|^{2H} + |s|^{2H} - |t-s|^{2H}), \quad (1)$$

where $\mathscr{E}$ stands for the expectation operator.

It follows from the above equation that the variance of fBm is of the type

$$\mathrm{var}(B_H(t)) = \sigma^2 |t|^{2H}. \quad (2)$$

As a nonstationary process, fBm does not admit a spectrum in the usual sense. However, it is possible to attach to it an average spectrum [29] [8]

$$\mathscr{S}_{B_H}(\omega) = \frac{\sigma^2}{|\omega|^{2H+1}}. \quad (3)$$

It is this power-law behavior of fBm's average spectrum which makes it attractive for modeling stochastic processes with long-term dependencies, such as $1/f$-type processes.

Although nonstationary, fBm does have stationary increments, which means that the probability properties of the process $B_H(t+s) - B_H(t)$ only depend on the lag variable s. Moreover, this increment process is self-similar in the sense that, for any $a > 0$ (and with the convention $B_H(0) = 0$), we get

$$B_H(at) \overset{\mathrm{d}}{=} a^H B_H(t), \quad (4)$$

where $\overset{\mathrm{d}}{=}$ means equality in distribution.

This self-similarity, which is inherent to the fBm structure, has the consequence that one individual realization of such a process is a fractal curve. It has, therefore, a fractal (i.e., noninteger) dimension which turns out to be [19] [7]

$$D = 2 - H. \quad (5)$$

According to the possible values of H, it follows that $1 < D < 2$, the scalar fBm parameter H being related to the roughness of fBm samples.

III. Second-Order Statistics of fBm Wavelet Coefficients

It is clear from the previous section that two important features are to be taken into account when analyzing fBm

- *nonstationarity*, which necessitates some *time-dependent* analysis;
- *self-similarity*, which necessitates some *scale-dependent* analysis.

As a result, wavelet analysis [5] which, by nature, is a time-scale method, appears as a natural tool and second-order wavelet analysis of fBm will now be carried out.

Manuscript received February 1, 1991; revised August 2, 1991. This work was presented at the IMA Conference on Wavelets, Fractals, and Fourier Transforms, Cambridge, England, December 1990.

The author was with LTS-ICPI, Lyon. He is now with Ecole Normale Supérieure du Lyon, Laboratoire de Physique (URA 1325 CNRS), 46 Allée d'Italie 69364, Lyon Cedex 07, France.

IEEE Log Number 9104354.

0018-9448/92$03.00

A. Orthonormal Wavelet Decompositions

Let us consider a discrete orthonormal wavelet decomposition of a given fBm $B_H(t)$. By definition, computing the corresponding wavelet coefficients amounts to evaluating [18], [21]

$$d_j[n] = 2^{-j/2} \int_{-\infty}^{+\infty} B_H(t) \psi(2^{-j}t - n)\, dt, \qquad j \in Z, \quad n \in Z, \quad (6)$$

where $\psi(t)$ is the basic wavelet, required to satisfy the admissibility condition [12]

$$\int_{-\infty}^{+\infty} \psi(t)\, dt = 0. \quad (7)$$

The simplest example of an orthonormal wavelet basis is provided by the Haar system for which

$$\psi(t) = \begin{cases} +1, & 0 \le t < 1/2, \\ -1, & 1/2 \le t < 1, \\ 0, & \textit{otherwise}. \end{cases} \quad (8)$$

For any given resolution 2^J, the wavelet mean-square representation of fBm is

$$B_H(t) = 2^{-J/2} \sum_{n=-\infty}^{+\infty} a_J[n] \phi(2^{-J}t - n) + \sum_{j=-\infty}^{J} 2^{-j/2} \sum_{n=-\infty}^{+\infty} d_j[n] \psi(2^{-j}t - n), \quad (9)$$

where equality is to be understood in a mean-square sense and where the *approximation* coefficients

$$a_j[n] = 2^{-j/2} \int_{-\infty}^{+\infty} B_H(t) \phi(2^{-j}t - n)\, dt \quad (10)$$

are computed with the help of the "scaling function" $\phi(t)$ associated with $\psi(t)$ [18], [21]. In this picture, the wavelet coefficients have an interpretation in terms of *details*, i.e., of difference in information between two successive approximations.

Instead of directly evaluating wavelet coefficients *via* the inner product (6), it is possible to recursively compute them by means of cascaded discrete filters [18]. Starting from an initial sequence $a_0[n]$ at a given resolution, successive sequences of approximations $a_j[n]$ and details $d_j[n]$ at lower resolutions obey the following recursions

$$a_j[n] = \sum_{n'=-\infty}^{+\infty} h[2n - n'] a_{j-1}[n']; \quad (11)$$

$$d_j[n] = \sum_{n'=-\infty}^{+\infty} g[2n - n'] a_{j-1}[n'], \quad (12)$$

where $h[n]$ and $g[n]$ stand for the coefficients of the discrete filters associated respectively with the scaling function $\phi(t)$ and the associated wavelet $\psi(t)$. (In the case of the Haar system, only two nonzero coefficients are needed: $h[0] = h[1] = g[0] = -g[1] = 1/\sqrt{2}$.)

This decomposition allows a perfect reconstruction [18], according to the following recursion

$$a_j[n] = \sum_{n'=-\infty}^{+\infty} h[2n' - n] a_{j+1}[n'] + \sum_{n'=-\infty}^{+\infty} g[2n' - n] d_{j+1}[n'], \quad (13)$$

provided that an initial (coarser) approximation $a_J[n]$ and the different sequences of details $d_j[n]$ at finer scales $j \le J$ are given.

B. Correlation and Stationarity

For each scale 2^j, the wavelet coefficients $d_j[n]$ form a discrete sequence of random coefficients but, although the family $\{2^{-j/2}\psi(2^{-j}t - n),\ j \in Z,\ n \in Z\}$ constitutes an orthonormal system, there is *a priori* no reason for the wavelet coefficients to be uncorrelated. Using (1), (6) and (7), a straightforward calculation yields

$$\mathscr{E}(d_j[n] d_k[m]) = \frac{\sigma^2}{2}\left(-\int_{-\infty}^{+\infty} A_\psi(2^{j-k}, \tau - (2^{j-k}n - m)) |\tau|^{2H}\, d\tau\right)(2^k)^{2H+1}, \quad (14)$$

where

$$A_\psi(\alpha, \tau) = \sqrt{\alpha} \int_{-\infty}^{+\infty} \psi(t) \psi(\alpha t - \tau)\, dt \quad (15)$$

is the so-called *wide-band ambiguity function* of $\psi(t)$ [9] or, equivalently, the *reproducing kernel* of the analysis, i.e., the wavelet transform of the wavelet itself [12].

From the general result (14), we can deduce the following Theorem (the proof of which is straightforward)

Theorem 1: When normalized according to $\tilde{d}_j[n] = (2^j)^{-(H+1/2)} d_j[n]$, wavelet coefficients of fBm give rise to

- time sequences which are self-similar and stationary in the sense that, for any j, $\mathscr{E}(\tilde{d}_j[n] d_j[m])$ is a unique function of $n - m$, namely

$$\mathscr{E}(\tilde{d}_j[n] \tilde{d}_j[m]) = \frac{\sigma^2}{2}\left(-\int_{-\infty}^{+\infty} \gamma_\psi(\tau - (n - m)) |\tau|^{2H}\, d\tau\right), \quad (16)$$

  with $\gamma_\psi(\tau) = A_\psi(1, \tau)$;
- scale sequences which are stationary in the sense that, for any n and $m = 2^{j-k}n$ associated to synchronous time instants, $\mathscr{E}(\tilde{d}_j[n] \tilde{d}_k[m])$ is a unique function of $j - k$, namely

$$\mathscr{E}(\tilde{d}_j[n] \tilde{d}_k[2^{j-k}n]) = \frac{\sigma^2}{2}\left(-\int_{-\infty}^{+\infty} A_\psi(2^{j-k}, \tau) |\tau|^{2H}\, d\tau\right) \cdot (2^{j-k})^{-(H+1/2)}. \quad (17)$$

(It should be noted that both results have already been established in the case of continuous wavelet transforms, the former in [8] and the latter in [25].)

If self-similarity and scale stationarity seem quite natural, *time* stationarity of wavelet coefficients of fBm deserves some comment. Time stationarity is in fact obtained because the basic "mother" wavelet $\psi(t)$ has a mean value which must necessarily be zero because of the admissibility condition (7). This indicates that the essential cause of nonstationarity of fBm turns out to be concentrated around the zero frequency and, hence, cannot be revealed by a fundamentally band-pass analysis. Nevertheless, the low-frequency nonstationarity of fBm can be characterized if the analysis also considers the companion "father" wavelet $\phi(t)$ (the low-pass "scaling function") associated to $\psi(t)$ [18], [21]. We, thus, obtain

$$\operatorname{var}(a_j[n]) = \frac{\sigma^2}{2}\left(-\int_{-\infty}^{+\infty}(\gamma_\phi(\tau) - 2\phi(\tau - n))\,|\tau|^{2H}\,d\tau\right)(2^j)^{2H+1}, \tag{18}$$

which is now a self-similar, but *time-dependent*, quantity. In other words, details are stationary, while approximations are not.

From (16), we have access to the variance of wavelet coefficients, namely

$$\operatorname{var}(d_j[n]) = \frac{\sigma^2}{2}V_\psi(H)(2^j)^{2H+1}, \tag{19}$$

where the constant $V_\psi(H)$, which depends on both the chosen wavelet and the fBm index, is defined by

$$V_\psi(H) = -\int_{-\infty}^{+\infty}\gamma_\psi(\tau)\,|\tau|^{2H}\,d\tau. \tag{20}$$

It follows from the power-law behavior (19) of the wavelet coefficients' variance that

$$\log_2(\operatorname{var}(d_j[n])) = (2H+1)j + \text{constant}. \tag{21}$$

Therefore, the fBm index H (and hence the associated fractal dimension D) can be easily obtained from the slope of this variance plotted as a function of scale in a log-log plot [18].

C. Approximate Whitening Filters

We have mentioned that, in general, the wavelet coefficients of fBm are correlated in both time and scale. However, it would be interesting to evaluate how strong this correlation is, or even to point out special cases for which decorrelation could be achieved. In such a case, the wavelet decomposition would provide us with a Kahrunen–Loève-type expansion [27] and it would then play the role of a whitening filter especially adapted to self-similar processes.

It turns out that the simplest orthonormal wavelet system, i.e., the Haar system, approaches such a doubly orthogonal decomposition when $H = 1/2$, i.e., for ordinary Brownian motion. More precisely, the following result holds.

Theorem 2: Let $d_j[n]$, $j \in Z$, $n \in Z$ be the Haar coefficients associated with ordinary Brownian motion (i.e., fBm with $H = 1/2$). If we fix a given time-scale index (n, j) and if we consider the correlation of $d_j[n]$ with Haar coefficients at finer scales $k \le j$, we have

$$\mathscr{E}(d_j[n]\,d_k[m]) = 0 \tag{22}$$

only outside of the (cone-shaped) time-scale domain defined by indexes (m, k) such that $2^{j-k}n \le m \le 2^{j-k}(n+1) - 1$. Moreover, we get for each scale

$$\mathscr{E}(d_j[n]\,d_j[m]) = \operatorname{var}(d_j[n])\,\delta_{nm} \tag{23}$$

and the correlation in scale varies as $2^{5(k-j)/2}$, for synchronous time instants.

Proof: It is first convenient to rewrite the correlation between wavelet coefficients as

$$\mathscr{E}(d_j[n]\,d_k[m]) = \frac{\sigma^2}{2}2^{(j+k)/2}(2^k)^{2H} \cdot \int_{-\infty}^{+\infty}\psi(t)\Theta_\psi(2^{j-k}(t+n) - m; H)\,dt, \tag{24}$$

with

$$\Theta_\psi(t; H) = -\int_{-\infty}^{+\infty}\psi(t-\tau)\,|\tau|^{2H}\,d\tau. \tag{25}$$

In the case of the Haar system (8), it can be shown that

$$\Theta_\psi(t; 1/2) = \begin{cases} 1/4, & t < 0, \\ 1/4 - t^2, & 0 \le t < 1/2, \\ (t-1)^2 - 1/4, & 1/2 \le t < 1, \\ -1/4, & t \ge 1. \end{cases} \tag{26}$$

Therefore, provided that the condition $k \le j$ is satisfied, the non-constant part of $\Theta_\psi(t; 1/2)$ is restricted in time to the interval $2^{k-j}m - n \le t \le 2^{k-j}(m+1) - n$ and, hence, the integral involved in the computation of $\mathscr{E}(d_j[n]d_k[m])$ is nonzero for all indexes such that this time interval has some overlap with the nonzero part of the Haar wavelet, i.e., with the interval [0, 1]. This results in the range $2^{j-k}n \le m \le 2^{j-k}(n+1) - 1$.

If we now fix $k = j$, the previous inequality reduces to $m = n$. This indicates that, at a given scale, distinct Haar coefficients of Brownian motion are uncorrelated with, moreover,

$$\operatorname{var}(d_j[n]) = \frac{\sigma^2}{2}\frac{1}{6}2^{2j}. \tag{27}$$

This is the second result of Theorem 2.

If we are now interested in correlations in scale ($k < j$), we can fix a given time index, say n, and compare $d_j[n]$ with other wavelet coefficients $d_k[m]$, which are synchronous in time. This amounts to consider time indexes m such that $m = 2^{j-k}n$ and it is then easy to show that

$$\int_{-\infty}^{+\infty}\psi(t)\Theta_\psi(2^{j-k}(t+n) - m; 1/2)\,dt = 2^{k-j}, \tag{28}$$

from which we get

$$\mathscr{E}(d_j[n]\,d_k[2^{j-k}n]) = \frac{\sigma^2}{2}\frac{1}{4}2^{2j}2^{5(k-j)/2}, \tag{29}$$

whence the last result. □

The Haar system does not provide, *stricto sensu*, a doubly orthogonal decomposition of ordinary Brownian motion. However, we can conclude from Theorem 2 that the correlation between distinct Haar coefficients decays as a power-law of scale and is zero for a given scale. We will now consider possible extensions of this behavior by retaining the Haar system as the wavelet basis while replacing the particular value $H = 1/2$ by different values in the range $0 < H < 1$.

For a given scale 2^j and for $|n - m| \geq 1$, a direct calculation yields

$$\mathscr{E}(d_j[n]d_j[m]) = \frac{\sigma^2}{2}\frac{1}{(2H+1)(2H+2)}\xi[n-m](2^j)^{2H+1}, \quad (30)$$

with

$$\xi[n] = (|n|-1)^{2H+2} - 4(|n|-1/2)^{2H+2} + 6|n|^{2H+2} - 4(|n|+1/2)^{2H+2} + (|n|+1)^{2H+2}, \quad (31)$$

and the corresponding constant (20) is

$$V_\psi(H) = \frac{1-2^{-2H}}{(H+1)(2H+1)}. \quad (32)$$

The behavior of this correlation function of Haar coefficients is depicted in Fig. 1 for different values of the fBm index within the range $0 < H < 1$. It reveals in fact three different regimes associated to the three possible situations $0 < H < 1/2$, $H = 1/2$ and $1/2 < H < 1$. The first two cases correspond, respectively, to an approximate decorrelation (fast decay) and a perfect decorrelation (only one nonzero coefficient), whereas the last one is associated with a long-term correlation (slow decay). This last point can be checked from the closed-form expression (31) of the Haar coefficients' correlation, since a fourth-order expansion in $1/|n|$ for (30) results in the asymptotic behavior

$$\mathscr{E}(d_j[n]d_j[m]) \sim O(|n-m|^{2(H-1)}) \quad (33)$$

when $|n - m| \gg 1$.

Another way of looking at the decay properties of the coefficients' correlation is to adopt a frequency point of view. Since we have from (16)

$$\mathscr{E}(d_j[n]d_j[m]) = \frac{\sigma^2}{2}\left(2\sin(\pi H)\Gamma(2H+1) \cdot \int_{-\infty}^{+\infty} e^{i\omega(n-m)}\frac{|\Psi(\omega)|^2}{|\omega|^{2H+1}}\frac{d\omega}{2\pi}\right)(2^j)^{2H+1}, \quad (34)$$

where $\Psi(\omega)$ is the Fourier transform of $\psi(t)$, it is clear that the decay of the correlation heavily depends on the behavior of $\Psi(\omega)$ at the zero frequency, and, hence, on the number of vanishing moments of $\psi(t)$.

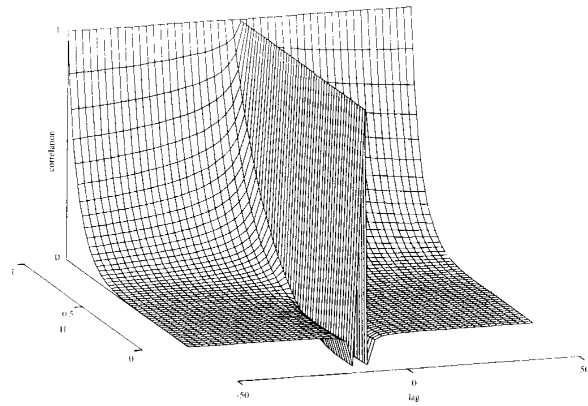

Fig. 1. Correlation of Haar coefficients for continuous-time fBm. At a given scale, the correlation of Haar coefficients is given by (30)–(31). The (normalized) result is plotted here for a number of fBm indexes H. Range $0 < H < 1/2$ corresponds to an approximate decorrelation (fast decay). Perfect decorrelation (only one nonzero coefficient) is achieved for $H = 1/2$ whereas the range $1/2 < H < 1$ is associated to a long-term correlation (slow decay).

More precisely, if $\psi(t)$ has at most R vanishing moments, i.e., if

$$\int_{-\infty}^{+\infty} t^r\psi(t)\,dt = 0, \qquad r \leq R, \quad (35)$$

then it is not possible to prevent divergence of $|\Psi(\omega)|^2|\omega|^{-(2H+1)}$ at the zero frequency if the fBm index H is such that

$$H > R - 1/2. \quad (36)$$

As a consequence, the correlation of the corresponding wavelet coefficients has a slow decay and the asymptotic behavior

$$\mathscr{E}(d_j[n]d_j[m]) \sim O(|n-m|^{2(H-R)}) \quad (37)$$

when $|n - m| \gg 1$. This is exactly what happens in the Haar case $R = 1$ for which the associated divergence situation corresponds to the fBm range $1/2 < H < 1$.

Nevertheless, as soon as a wavelet with $R \geq 2$ is chosen, the quantity $R - 1/2$ is ensured to exceed the maximum value of H within its range, i.e., 1. Therefore, it is to be expected that the pathological situation of a slow decay of the wavelet coefficients' correlation, which results jointly from the low regularity of the Haar system and from a particular range of H, will be overcome for more regular choices (e.g., any Daubechies' wavelet [6] such that $R \geq 2$). As proved by Tewfik and Kim [24], it turns out that this guess is true and that the number of vanishing moments directly controls the correlation at a given scale and between scales, large R's leading to almost uncorrelated coefficients. (A simulation illustrating this fact is given in [10].)

D. Discrete Evaluations and Sampling

Let us suppose now that we are given a discrete sequence considered as an initial approximation at the best available resolution. If this initial approximation is obtained from a continuous-time fBm $B_H(t)$ as

$$\hat{a}_0[n] = \int_{-\infty}^{+\infty} B_H(t)\phi(t-n)\,dt, \tag{38}$$

it follows from the linear transformations involved in the wavelet decomposition that the coefficients' recursions (11)–(12) give rise to related recursions concerning coefficients' correlations. Applying (11)–(12) to the discrete sequence (38) yields the following results

- the approximation coefficients are such that

$$\mathscr{E}(\hat{a}_j[n]\hat{a}_j[m]) = \frac{\sigma^2}{2}(A_j[n] + A_j[m] - D_j[n-m]), \tag{39}$$

with

$$A_0[n] = \int_{-\infty}^{+\infty} \phi(\tau - n)\,|\tau|^{2H}\,d\tau; \tag{40}$$

$$A_j[n] = \sqrt{2}\sum_{n'=-\infty}^{+\infty} h[2n-n']\,A_{j-1}[n'],\ j \geq 1 \tag{41}$$

and

$$D_0[n] = \int_{-\infty}^{+\infty} \gamma_\phi(\tau - n)\,|\tau|^{2H}\,d\tau \tag{42}$$

$$D_j[n] = \sum_{n'=-\infty}^{+\infty} \gamma_h[2n-n']\,D_{j-1}[n'],\ j \geq 1; \tag{43}$$

- the detail coefficients are such that

$$\mathscr{E}(\hat{d}_j[n]\hat{d}_j[m]) = \frac{\sigma^2}{2}C_j[n-m], \tag{44}$$

with

$$C_j[n] = -\sum_{n'=-\infty}^{+\infty} \gamma_g[2n-n']\,D_{j-1}[n'],\ j \geq 1, \tag{45}$$

where $\gamma_h[n]$ and $\gamma_g[n]$ are the discrete-time autocorrelation functions of the impulse responses of the filters $h[n]$ and $g[n]$, respectively,

$$\gamma_h[n] = \sum_{n'=-\infty}^{+\infty} h[n']\,h[n'-n]; \tag{46}$$

$$\gamma_g[n] = \sum_{n'=-\infty}^{+\infty} g[n']\,g[n'-n]. \tag{47}$$

Because, by construction of $\hat{a}_0[n]$, $B_H(t)$ has been forced to live in an approximation space V_0 spanned by $\{\phi(t-n),\ n \in Z\}$ and has been sampled accordingly, there is no difference between the coefficients $\hat{a}_j[n]$ and $\hat{d}_j[n]$ on one hand, and the $a_j[n]$ and $d_j[n]$ considered previously on the other hand. However, if the discrete sequence $\hat{a}_0[n]$ now corresponds to a *sampled* fBm [17], i.e., is such that

$$\hat{a}_0[n] = B_H(nT_s), \tag{48}$$

where T_s is some sampling period which can be chosen arbitrarily as unity, the situation is quite different. Obviously, aliasing problems occur when defining such a discrete-time process, and the corresponding sequences of approximations $\hat{a}_j[n]$ and details $\hat{d}_j[n]$ now differ from the $a_j[n]$ and $d_j[n]$ deduced from the continuous-time process.

Nevertheless, it can be shown that (39) and (44) still hold, provided that the initializations (40) and (42) of the recursions (41), (43), and (45) are changed according to

$$A_0[n] = D_0[n] = |n|^{2H}. \tag{49}$$

As a consequence, the power-law behavior (19) of the wavelet coefficients' variance is generally modified. In particular, it can be shown that, in the case of the Haar system, the variance of $\hat{d}_j[n]$ is still of the form (19), but with the constant $V_\psi(H)$ replaced by a scale-dependent quantity. Precisely, we get

$$\operatorname{var}(\hat{d}_j[n]) = \frac{\sigma^2}{2}\tilde{V}_\psi(H,j)(2^j)^{2H+1}, \tag{50}$$

with

$$\tilde{V}_\psi(H,j) = 2^{-(j+2H)}\Bigg[1 + \sum_{m=1}^{2^{j-1}-1}(1-2^{1-j}m) \cdot \left(|1+2^{1-j}m|^{2H} - 2|2^{1-j}m|^{2H} + |1-2^{1-j}m|^{2H}\right)\Bigg]. \tag{51}$$

This results in an inequality

$$\operatorname{var}(\hat{d}_j[n]) \geq \operatorname{var}(d_j[n]) \tag{52}$$

according to which the "local" (scale-dependent) fractal dimension of a sampled fBm

$$D(j) = \log_2(\operatorname{var}(\hat{d}_{j+1}[n])) - \log_2(\operatorname{var}(\hat{d}_j[n])) \tag{53}$$

always exceeds that of its corresponding continuous-time counterpart (see Fig. 2(a)). Moreover, it turns out that the strength of the inequality is diminished when coarser scales are involved and/or when the fBm index H is increased. This can be explained if we consider the asymptotic behavior of (51) for large scale indices j. In this case, the quantity in brackets in (51) behaves approximately as

$$2^{j-1}\int_0^1 (1-x)\left[(1+x)^{2H} - 2x^{2H} + (1-x)^{2H}\right]dx = 2^j\frac{2^{2H}-1}{(H+1)(2H+1)} \tag{54}$$

and, therefore,

$$\lim_{j\to\infty}\tilde{V}_\psi(H,j) = V_\psi(H), \tag{55}$$

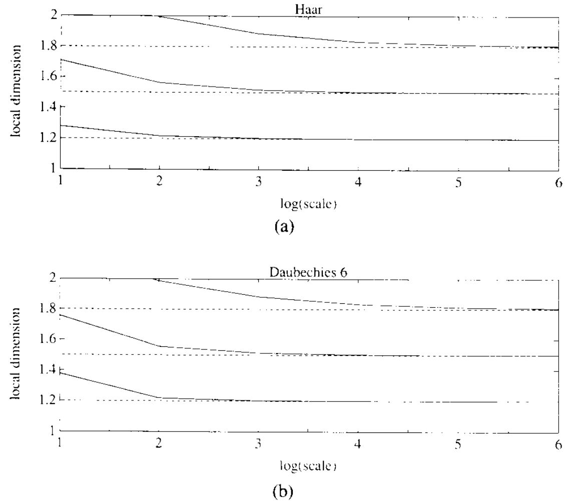

Fig. 2. Fractal dimension estimation for sampled fBm. In the case of sampled fBm, the variance of wavelet coefficients is given by (50)-(51). "Local" fractal dimensions are plotted (continuous lines) according to (53) and compared to the corresponding theoretical values (dotted lines) in three different cases: $D = 1.2$, $D = 1.5$, and $D = 1.8$. (a) Haar wavelet; (b) Daubechies wavelet with six vanishing moments.

with $V_\psi(H)$ as in (32). This means that the difference existing between the continuous and sampled cases is mostly concentrated at the finer scales and is progressively "forgotten" when coarser and coarser scales are involved.

If we fix now a given scale and if we allow H to vary, the convergence, as a Riemann sum, of the discrete sum in (51) to the integral (54) is accelerated if the function $|x|^{2H}$ is made smoother at $x = 0$, i.e., if H is increased: this is precisely the second effect observed. This behavior is not specific to the Haar system and is encountered as well in the case of wavelets with a higher number of vanishing moments. This is illustrated in Figure 2(b) where a Daubechies' wavelet with $R = 6$ has been chosen.

IV. Connection with Other Approaches

A. Analysis via Length Measurements

The question of estimating the spectral exponent of $1/f$-type processes, or even the fractal dimension of fBm, is not new. Various approaches have been proposed, most of which consider realizations of $1/f$-type processes as fractal curves whose length has to be measured. This is generally performed by means of some elementary ruler, the fractal dimension being deduced from the variation of this length as the length of the ruler is changed [19], [7].

An example related to such a measuring process is given by the so-called *Allan variance* [1]

$$v_A(T) = \frac{1}{2T^2}\,\mathcal{E}\left(\left[\int_{t-T}^{t} B_H(s)\,ds - \int_{t}^{t+T} B_H(s)\,ds\right]^2\right). \quad (56)$$

It can be easily shown that $v_A(T)$ does not depend upon t and varies as $O(T^{2H})$ as $T \to \infty$. A measure of fluctuation, corresponding to a measure of "length" of the signal considered as a curve, is obtained if the squared difference in (56) is replaced by an absolute value. Because of the Gaussianity of fBm, this results in a variation as $O(T^H)$ as $T \to \infty$.

It is clear that this kind of approach, which measures contributions of increments associated with increasingly smoothed processes, seems more or less equivalent to the evaluation of the standard deviation of Haar coefficients. This equivalence can be exactly quantified if we consider the discrete-time counterpart of Allan variance, as introduced by Burlaga and Klein [3], who consider a discrete-time sequence $\hat{a}_0[n]$ corresponding to data with the best available resolution. Increasingly smoothed versions are then constructed by locally averaging $\hat{a}_0[n]$ over nonoverlapping intervals of length k. For every such "scale" index k, a mean value of the (absolute value of the) corresponding increment process is finally computed.

More precisely, given a sequence $\hat{a}_0[n]$ of length N, what is evaluated by the algorithm of Burlaga and Klein is the following "length" function of k

$$L_{BK}[k] = \frac{1}{\left\lfloor \frac{N}{k} \right\rfloor k^3} \cdot \sum_{i=0}^{\left\lfloor \frac{N}{k} \right\rfloor - 1} \left| \sum_{n=0}^{k-1} \left(\hat{a}_0[n+ik] - \hat{a}_0[n+(i+1)k]\right)\right| \quad (57)$$

and what is expected is a behavior varying as k^{-D}, where $D = 2 - H$ is the fractal dimension.

This definition allows us to establish the following general result.

Theorem 3: When evaluated at dyadic scales, the average "length" (in the sense of Burlaga and Klein) of a Gaussian sequence with stationary increments is proportional to the standard deviation of the corresponding Haar coefficients.

Proof: Let us assume for convenience that $N = 2^K$. Using the stationarity of increments, we have then, for dyadic scales $k = 2^{j-1}$,

$$\mathcal{E}\left(L_{BK}[2^{j-1}]\right) = 2^{3-2j-K} \sum_{n=1}^{2^{K-j}} \mathcal{E}\left(\left|\sum_{m=0}^{2^{j-1}-1} \left(\hat{a}_0[m+2^{j-1}(2n)] - \hat{a}_0[m+2^{j-1}(2n-1)]\right)\right|\right). \quad (58)$$

On the other hand, if we consider Haar coefficients $\hat{d}_j[n]$ associated to $\hat{a}_0[n]$, we have

$$\hat{d}_j[n] = \frac{1}{\sqrt{2}}\left(\hat{a}_{j-1}[2n] - \hat{a}_{j-1}[2n-1]\right), \quad (59)$$

with

$$\hat{a}_j[n] = \frac{1}{\sqrt{2}}\left(\hat{a}_{j-1}[2n] + \hat{a}_{j-1}[2n-1]\right). \quad (60)$$

Therefore, by induction, we end up with

$$\hat{d}_j[n] = 2^{-j/2} \sum_{m=0}^{2^{j-1}-1} \left(\hat{a}_0[2^{j-1}(2n) - m] - \hat{a}_0[2^{j-1}(2n-1) - m]\right) \quad (61)$$

and, using again the stationarity of fBm increments,

$$\mathscr{E}\left(\left|\sum_{m=0}^{2^{j-1}-1} \left(\hat{a}_0[m + 2^{j-1}(2n-1)] - \hat{a}_0[m + 2^{j-1}(2n)]\right)\right|\right) = 2^{j/2}\mathscr{E}(|\hat{d}_j[n]|). \quad (62)$$

Using finally the Gaussianity of fBm, it follows from (58) and (62) that

$$\mathscr{E}(L_{BK}[2^{j-1}]) = 2^{3-5j/2}\sqrt{\frac{2}{\pi}}\sqrt{\operatorname{var}(\hat{d}_j[n])}. \quad \square \quad (63)$$

This equivalence can be used to explain the reported behavior [13] of the Burlaga–Klein estimate in the case of sampled fBm. According to (50) and (51), the average length (63) is proportional to $(2^{j-1})^{-D}$ only for large j's, and not for all of them, as expected. As a consequence, the scale dependence of the local fractal dimension leads to overestimated D's [13], [11].

B. Synthesis via Dyadic Interpolation

The wavelet analysis carried out in the previous sections can be thought of as a decomposition from which perfect reconstruction can be achieved. This suggests, therefore, to use such a reconstruction as a *synthesis* tool, provided that its inputs have identical statistical properties to that of the coefficients deduced from the analysis.

As suggested by Wornell [27] and as validated by the results of Section III-C, a convenient simplification is to ignore the correlation which exists between different wavelet coefficients. Considering then a collection of uncorrelated Gaussian coefficients $d_j[n]$ such that

$$\operatorname{var}(d_j[n]) = \sigma^2(2^j)^{2H+1}, \quad (64)$$

i.e., such that their variance follows precisely the power-law (19), Wornell has shown [27] that the process

$$\tilde{B}_H(t) = \lim_{J\to+\infty} \sum_{j=-\infty}^{J} 2^{-j/2} \sum_{n=-\infty}^{+\infty} d_j[n]\psi(2^{-j}t - n) \quad (65)$$

has a time-averaged spectrum $\mathscr{S}_{\tilde{B}_H}(\omega)$ that satisfies

$$\gamma_1 \frac{\sigma^2}{|\omega|^{2H+1}} \le \mathscr{S}_{\tilde{B}_H}(\omega) \le \gamma_2 \frac{\sigma^2}{|\omega|^{2H+1}}, \quad (66)$$

where γ_1 and γ_2 are constants depending on $\psi(t)$. Therefore, wavelets offer a new possibility for synthesizing nearly-$1/f$-type and, hence, fBm-like processes. It is worthwhile to point out that the idea of constructing a self-similar function by adding up finer and finer details, all similar except for scale, is not new: it is even the essence of basic fractal constructions. Nevertheless, in this case too, wavelets provide new insights on such approaches and allow us to get a better understanding of some limitations of more conventional techniques.

In this regard, a popular method for constructing random fractals approximating fBm is the so-called *random midpoint displacement method* [23]. Its principle is the following[1]: given an initial interval [0, 1], the value at 0 is set to 0 and that at 1 is selected as a sample of a Gaussian variable with a given variance σ^2. The interpolated value at $1/2$ is then constructed as the average of the values at 0 and 1 plus an offset selected as a sample from a Gaussian distribution with variance $\sigma^2/2^{2H+1}$, and the procedure is iterated. This fails however to provide stationary increments when $H \neq 1/2$ and the resulting process is only an approximation of a fBm [23]. In any case, the random midpoint displacement method can be given a wavelet interpretation. It can be easily seen that it fits into the framework (13), provided that the discrete filters $h[n]$ and $g[n]$ are defined with the only nonzero coefficients being $h[0] = 1$, $h[-1] = h[1] = \frac{1}{2}$ and $g[1] = 1$. Unfortunately, this does not give rise to an orthonormal system [6] and, even if uncorrelated coefficients are used as inputs, fBm-type behavior cannot be guaranteed as is possible for an orthonormal system.

Returning to Wornell's orthonormal synthesis (65), we can remark that the result in (66) requires no assumption on the particular order of $h[n]$ giving rise to $\psi(t)$, the desired fractal structure of the synthesized process stemming only from the variance power-law (64). However, it is known [6] that the number of vanishing moments of a wavelet is also related to its *regularity*. In particular, if $R = 2$, the Daubechies' wavelet turns out to be fractal itself [6] and it is expected that the corresponding synthesized process should exhibit fractal properties mixing those of the construction algorithm and of the elementary building blocks on which the synthesis relies. In this respect, large R's should improve fBm synthesis, both for validating the assumption of decorrelation between coefficients (cf. Section III-C) and for rendering the influence of the wavelet regularity negligible. Let us remark that interconnections between R and the variance power-law of wavelet coefficients have also been considered by Cohen [4] who stated that, if a process whose power spectrum is bounded (up to a constant) by $|\omega|^{-(2H+1)}$ is analyzed with a wavelet with R vanishing moments and $R > H - 1$, the variance of the corresponding wavelet coefficients is bounded (up to a constant) by $(2^j)^{2H+1}$. This is, however, of little consequence for fBm-like processes (65) with $0 < H < 1$, since the above inequality is then satisfied for any $R \geq 0$ (this always holds because of the admissibility condition).

V. Conclusion

A number of results have been provided for characterizing, analyzing or synthesizing fBm *via* wavelets. Beyond the mere results, the wavelet point of view has proven useful for incorporating previous methods devoted to fBm into a general framework and for evaluating and generalizing them. Moreover, some of the most promising uses of this framework are as the basis for actually solving signal processing problems such as detection in $1/f$ background noise, estimation of fractal dimensions or multiscale optimal filtering (see e.g., [28], [15], or [11]).

One of the key reasons for which wavelets are well fitted to fBm is the self-similarity of such a process. Strictly speaking, this self-similarity is *global* in the sense that scaling laws are supposed to hold uniformly at all scales and fractal dimension is not allowed to change with time. From a physical point of view, this can be too strong an idealization and it could be desirable to account for modifications of the model allowing *multifractal* [19] or *locally self-similar* situations. It is believed that, in this direction too,

[1] In fact, motivation for this construction can be traced back to [16] or [26].

wavelets offer a promising and flexible tool, as early attempts indicate [2], [25], [22].

Acknowledgment

Useful discussions with N. Gache, E. Payot, O. Rioul, G. Ruckebush, and within the Rennes Working Group "Analyse multirésolution de signaux aléatoires" (M. Basseville and A. Benveniste) are gratefully acknowledged.

References

[1] D. W. Allan, "Statistics of atomic frequency clocks," *Proc. IEEE*, vol. 54, no. 2, pp. 221-230, 1966.

[2] E. Bacry, A. Arnéodo, U. Frisch, Y. Gagne, and E. Hopfinger, "Wavelet analysis of fully developed turbulence data and measurement of scaling exponents," in *Turbulence and Coherent Structures*, O. Métais and M. Lesieur, Eds. New York: Kluwer, 1991, pp. 203-215.

[3] L. F. Burlaga and L. W. Klein, "Fractal structure of the interplanetary magnetic field," *J. Geophys. Res.*, vol. 91, no. A1, pp. 347-350, 1986.

[4] A. Cohen, "Ondelettes, Analyses Multirésolutions et Traitement Numérique du Signal," thése de Doctorat, Univ. Paris IX, Dauphine, 1990.

[5] J. M. Combes, A. Grossmann and Ph. Tchamitchian, Eds., Wavelets. New York: Springer-Verlag, 1989.

[6] I. Daubechies, "Orthonormal bases of compactly supported wavelets," *Comm. Pure Appl. Math.*, vol. XLI, no. 7, pp. 909-996, 1988.

[7] K. Falconer, *Fractal Geometry*, Chichester: J. Wiley and Sons, 1990.

[8] P. Flandrin, "On the spectrum of fractional Brownian motions," *IEEE Trans. Inform. Theory*, vol. 35, pp. 197-199, Jan. 1989.

[9] P. Flandrin, "Some aspects of nonstationary signal processing with emphasis on time-frequency and time-scale methods," in [5], pp. 68-98, 1989.

[10] P. Flandrin, "Fractional Brownian motion and wavelets," to appear in *Wavelets, Fractals and Fourier Transforms - New Developments and New Applications*, M. Farge, J. C. R. Hunt and J. C. Vassilicos, Eds. Oxford: Oxford Univ. Press.

[11] N. Gache, P. Flandrin, and D. Garreau, "Fractal dimension estimators for fractional Brownian motions," in *IEEE Int. Conf. Acoust., Speech and Signal Processing, ICASSP-91*, Toronto, pp. 3557-3560, 1991.

[12] A. Grossmann and J. Morlet, "Decomposition of Hardy functions into square integrable wavelets of constant shape," *SIAM J. Math. Anal.*, vol. 15, no. 4, pp. 723-736, 1984.

[13] T. Higuchi, "Approach to an irregular time series on the basis of the fractal theory," *Physica D*, vol. 31, pp. 277-283, 1988.

[14] M. S. Keshner, "$1/f$ noise," *Proc. IEEE*, vol. 70, pp. 212-218, 1982.

[15] M. Kim and A. H. Tewfik, "Multiscale signal detection in fractional Brownian motion," in *Advanced Signal Processing Algorithms, Architectures and Implementations*, F. T. Luk, Ed., also in *SPIE*, vol. 1348, pp. 462-470, 1990.

[16] P. Lévy, "Le Mouvement Brownien," *Mém. Sc. Math.*, fasc. 126, pp. 1-81, 1954.

[17] T. Lundahl, W. J. Ohley, S. M. Kay, and R. Siffert, "Fractional Brownian motion: A maximum likelihood estimator and its application to image texture," *IEEE Trans. Med. Imaging*, vol. MI-5, no. 3, pp. 152-161, 1986.

[18] S. G. Mallat, "A theory for multiresolution signal decomposition: the wavelet representation," *IEEE Trans. Pattern Anal. Machine Intell.*, vol. PAMI-11, no. 7, pp. 674-693, 1989.

[19] B. Mandelbrot, *The Fractal Geometry of Nature*. Freeman: San Francisco, 1982.

[20] B. B. Mandelbrot and J. W. van Ness, "Fractional Brownian motions, fractional noises and applications," *SIAM Rev.*, vol. 10, no. 4, pp. 422-437, 1968.

[21] Y. Meyer, "Orthonormal wavelets," in *Wavelets*, J. M. Combes, A. Grossmann, and Ph. Tchamitchian, Eds. New York: Springer-Verlag, 1989, pp. 21-37.

[22] J. F. Muzy, E. Bacry, and A. Arnéodo, "Wavelets and multifractal formalism for singular signals: Application to turbulence data," preprint, 1991.

[23] H. O. Peitgen and D. Saupe, Eds., *The Science of Fractal Images*. New York: Springer-Verlag, 1988.

[24] A. H. Tewfik and M. Kim, "Correlation structure of the discrete wavelet coefficients of fractional Brownian motions," to appear in *IEEE Trans. on Inform. Theory*.

[25] M. Vergassola and U. Frisch, "Wavelet transforms of self-similar processes," to appear in *Physica D*.

[26] N. Wiener, *Nonlinear Problems in Random Theory*. Cambridge, MA: MIT Press, 1958.

[27] G. W. Wornell, "A Karhunen-Loève-like expansion for $1/f$ processes via wavelets," *IEEE Trans. Inform. Theory*, vol. 36, pp. 859-861, July 1990.

[28] G. W. Wornell and A. V. Oppenheim, "Estimation of fractal systems from noisy measurements using wavelets," to appear in *IEEE Trans. Signal Proc.*

[29] A. M. Yaglom, *Correlation Theory of Stationary and Related Random Functions*. New York: Springer-Verlag, 1986.

Application of the Wavelet Transform for Pitch Detection of Speech Signals

Shubha Kadambe and G. Faye Boudreaux-Bartels

Abstract—**An event detection pitch detector based on the dyadic wavelet transform is described. The proposed pitch detector is suitable for both low-pitched and high-pitched speakers and is robust to noise. Examples are provided that demonstrate the superior performance of this event based pitch detector in comparison with classical pitch detectors that use the autocorrelation and the cepstrum methods to estimate the pitch period.**

Index Terms—**Glottal closure, event, dyadic wavelet transform, pitch detection, local maxima.**

I. Introduction

The pitch period is an important parameter in the analysis and synthesis of speech signals. Pitch period information is used in various applications such as 1) speaker identification and verification, 2) pitch synchronous speech analysis and synthesis, 3) linguistic and phonetic knowledge acquisition and 4) voice disease diagnostics. The task of estimating the pitch period is very difficult since a) the human vocal tract is very flexible and its characteristics vary from person to person, b) the pitch period can vary from 1.25 ms to 40 ms, c) the pitch period of the same speaker can vary depending upon the emotional state of the speaker and d) the pitch period can be influenced by the way the word is pronounced (accent). Therefore, no one algorithm that has been developed so far performs perfectly for 1) different speakers (male, female, children and people with different native languages), 2) different applications and 3) different environmental conditions [1].

The pitch detectors that have been developed so far, can be broadly classified into either event detection pitch detectors or

Manuscript received February 15, 1991; revised September 1, 1991. This work was supported in part by ONR Grant #N00014-89-J-1812. This work was presented at the International Conference on Spoken Language Processing, Kobe, Japan, November 18, 1990, and at the Twenty-Fourth Annual Asilomar Conference on Signals, Systems, and Computers, Pacific Grove, CA, November 5-7, 1990.

S. Kadambe is with the Applied Science and Engineering Laboratories, A. I. duPont Institute, Wilmington, DE 19899.

G. F. Boudreaux-Bartels is with the Department of Electrical Engineering, University of Rhode Island, Kingston, RI 02881.

IEEE Log Number 9104511.

0018-9448/92$03.00